BAUXITE RESIDUE SINTER PHASE TRANSFORMATIONS

Harrison HODGE[1*], Pritii TAM[2], James VAUGHAN[1], Dimitris PANIAS[2]

[1] School of Chemical Engineering, University of Queensland, Australia
[2] National Technical University of Athens

h.hodge@uq.edu.au, pritii.tam@metal.ntua.gr, james.vaughan@uq.edu.au, panias@metal.ntua.gr*

Introduction

Bauxite residue (BR) contains between 2 and 35 wt% aluminium (expressed as Al_2O_3)[1]. This aluminium is lost from Bayer process, primarily due to the formation of sodium containing desilication products (DSP), incomplete digestion of aluminium bearing minerals and in some cases early precipitation of gibbsite. The sintering process has been used commercially in the processing of high silica bauxites and could be used effectively for the recovery of aluminium and sodium values from bauxite residue (BR). In the sinter process BR is calcined with Na_2CO_3 to produce a soluble $NaAlO_2$ product, while stabilising the silicates with CaO[2]. The recovery of this material is the first step in total BR valorisation. In this research, two distinct BRs' are characterised before and after sintering. The mineralogy was quantified using XDB[4,5]. Key reaction equilibrium was considered using the Factsage thermodynamic modelling package[5], contributing to the understanding of potential reaction pathways during sintering.

Experimental

Sintering was conducted at 900°C for 2 hours, in an air atmosphere. Between 20-30 minutes was taken to reach reaction temperature before being held for the reaction time and cooled in the furnace overnight. Two tests were completed per residue, one with CaO ((S + Ca AU/GR), 1 g BR: 0.25 g Na_2CO_3: 0.2 g CaO) and one without CaO ((S AU/GR), 1 g BR: 0.25 g Na_2CO_3). This amounts to molar ratios of 4.6 and 1.4 for the Greek BR and 1.4 and 2 for the Australian BR's for Ca:Si and Na:Al respectively. Factsage software was used to estimate equilibrium data for both observed and predicted reactions based on the outputs of the quantitative mineralogy as estimated by XDB software. XDB software uses a full-profile fit method where the measured spectra are fit to a composite of mineral standards in the database. To find an optimum peak fit and respect the mass balance, scale factors are applied. While this approach has limitations as the XDB database does not have a complete set of sinter product references, it provides a good indication of relative abundances of phases.

Results

Table 1 presents the BRs and sintered product composition (measured by XRF). Australian (AU) BR is high in sodium and silicon while Greek (GR) BR is high in calcium.

Table 1: Sample compositions (dry weight basis wt%,[1]Estimated LOI%)

Sample	Al_2O_3	CaO	Fe_2O_3	Na_2O	SiO_2	TiO_2	LOI
BR AU	18.5	1.7	42.0	9.0	15.3	6.4	6.2
BR GR	19.3	9.6	43.5	2.8	6.5	5.5	9.4
S AU	16.0	1.6	36.4	20.6	13.3	5.5	2.1
S GR	18.7	9.1	41.0	16.5	5.8	5.0	2.5[1]
S + Ca Au	14.3	14.8	32.2	18.3	12.1	4.9	2.5
S + Ca GR	16.3	19.7	36.0	14.5	5.1	4.4	2.5[1]

Figure 1 shows that the major differences between residues stem primarily from the aluminium-containing compounds, which is diaspore (α-AlOOH, **1**) and DSP (cancrinite ($Na_8(Al,Si)_{12}O_{24}(OH)_2.2H_2O$, **2**)) for GR BR. AU BR has mostly DSP (sodalite ($Na_4(Al,Si)_6O_{12}(OH)1.5H_2O$, **3**)) with minor boehmite (γ-AlOOH, **4**) and gibbsite ($Al(OH)_3$, **5**). Titanium in GR BR exists primarily as perovskite ($CaTiO_3$, **6**) compared to rutile and anatase (TiO_2, **7**) in AU BR. GR BR also contains grossular phases ($Ca_3FeAl(SiO_4)((OH)_4)_2$, **8**) which have no analogue in the AU sample.

Aluminium phases reacted to produced sodium aluminate ($NaAlO_2$, 9) or sodium aluminium silicate ($NaAlSiO_4$, **10**), with up to 70% of aluminium value recovered. In some cases (S Au and S GR), some residual DSP phases remained. Substantial hematite (Fe_2O_3, **11**) remained in all cases. In systems with no added CaO (with exception of existing calcite, $CaCO_3$, **12**), the formation of sodium ferrite ($NaFeO_2$, **13**) and ferro-titanate ($NaFeTiO_4$, **14**) was seen. Addition of CaO (**15**) reduced the presence of these compounds in favour of harmunite ($CaFeO_4$, **16**), Brownmillerite ($Ca_2Fe_2O_5$, **17**) and $CaTiO_3$. Calcium silicates were also formed (Ca_2SiO_4, Ca_3SiO_5, **18**). The unaccounted sodium and silicon was assumed to exist as amorphous Na_2O or SiO_2. A number of complex phases, notably garnet ($3(Ca,Fe,Mg)O(Al,Fe)_2O_3.3SiO_2$, **19**), were also detected.

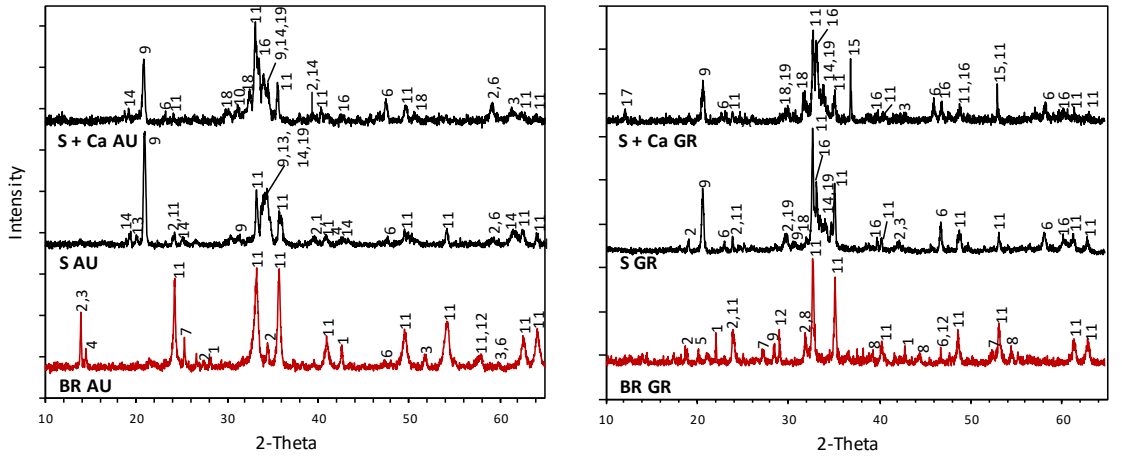

Figure 1: XRD patterns for both residues and all sinter products

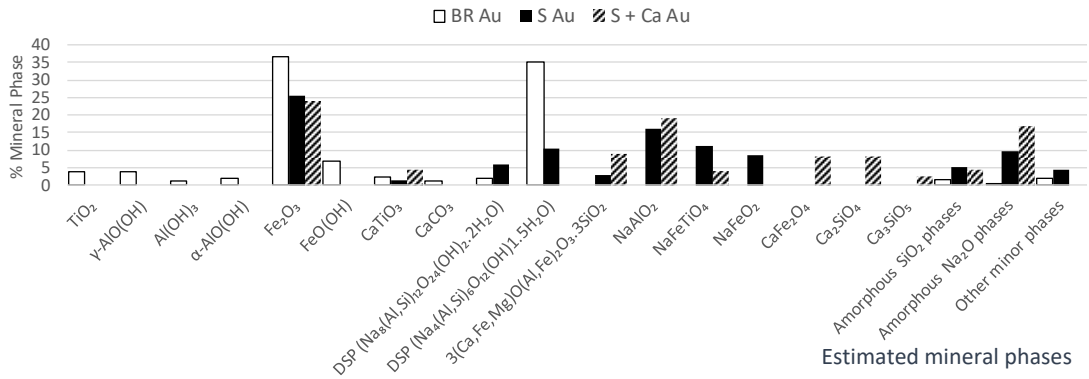

Figure 2: Estimated mineral phases from XDB for Australian BR and sinters

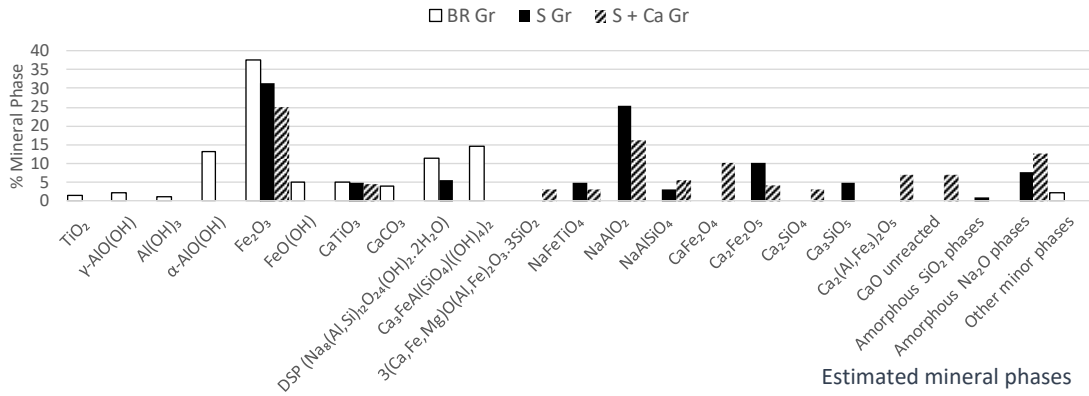

Figure 3: Estimated mineral phases from XDB for Greek BR and sinters

Outputs from XDB (AU and GR samples, Figure 2 and 3) indicate that $Al(OH)_3$ and AlOOH reacted directly with Na_2CO_3 (Equations (1) and (2)).

$$Na_2CO_3 + 2AlOOH \rightarrow 2NaAlO_{2(s)} + CO_{2(g)} + H_2O_{(g)} \quad (1)$$

$$Na_2CO_3 + 2Al(OH)_3 \rightarrow 2NaAlO_{2(s)} + CO_{2(g)} + 3H_2O_{(g)} \quad (2)$$

DSP reacts with CaO to produce Ca_2SiO_4 and $NaAlO_2$ (Equation (3)). This is expected to be the primary DSP reaction in GR residue. However, because of AU BR's naturally low CaO content, different reactions occur when only Na_2CO_3 is added, indicating an indirect reaction pathways. DSP phases are approximated as nepheline ($NaAlSiO_4$, Equation (3)) in Factsage due to database limitations as it mirrored major constituent elements of DSP in approximately the same ratios (Na:Al:Si = 1:1:1).

$$NaAlSiO_4 + 2CaO \rightarrow NaAlO_2 + Ca_2SiO_4 \quad (3)$$

CaO addition did not result in the formation of any additional $NaAlO_2$ in AU BR whereas there is reduction of $NaAlO_2$ formed in GR BR. The increased Ca: Si mole ratio, for the GR sinter mix, resulted in unwanted side reactions causing lower $NaAlO_2$. The formation of $CaFe_2O_4$ occurs via a two-stage process with $Ca_2Fe_2O_5$ formed first, while CaO is in abundance, followed by $CaFe_2O_4$.

Figure 4 depicts the sintering reactions observed in the sintering process. It should be noted that some minerals in the third row will also form when only Na_2CO_3 is added in GR sinters due to its high existing calcium content. Dotted lines indicate compounds which were detected but specific reactions could not be identified.

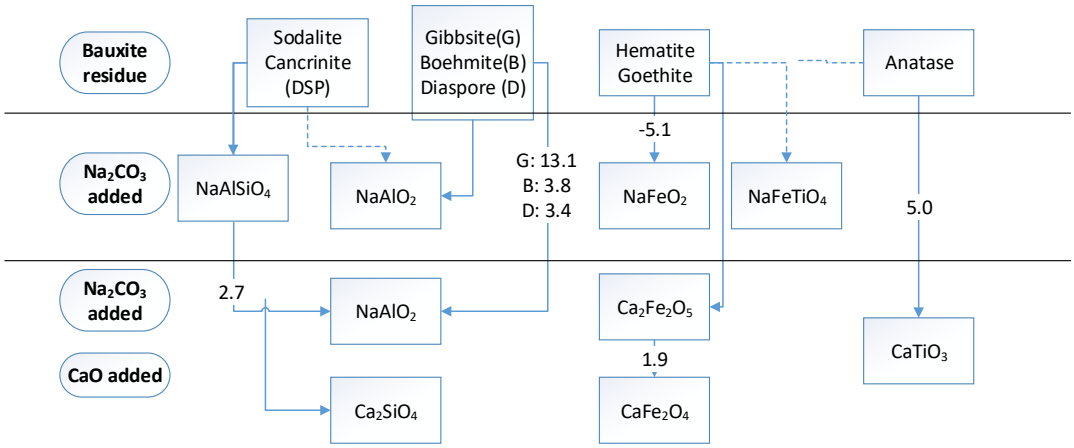

Figure 4: Map of potential reactions. Equilibrium constant presented as log K_{eq}

In summary, the incorporation of both thermodynamic study and quantitative mineralogical analysis can be useful to understand sinter mineral phase formations, though further works in optimising the sintering system should include changes to operating temperature and reagents dosages.

Acknowledgements

We acknowledge the funding by Rio Tinto and from European Community's Horizon 2020 Programme ([H2020/2014–2019]) under Grant Agreement no. 636876 (MSCA-ETN REDMUD, http://www.etn.redmud.org), as well as Aluminium of Greece for the support of this project. This publication reflects only the author's view, exempting the Community from any liability. Special thanks to Peter Hayes, William Hawker, Kelfin Hardiman, Warren Staker, Johannes Vind and Vicky Vasilliadou.

References

1. F. Kaussen, and B. Friedrich, "Soda Sintering Process for the Mobilisation of Aluminium and Gallium in Red Mud.", in *Bauxite Residue Valorisation and Best Practices (BR 2015)*, Leuven, Belgium, 2015.
2. C. Klauber, M. Grafe and G. Power, "Bauxite residue issues: II. Options for Residue Utilization" Hydrometallurgy, **108** (1-2) 11-32 (2011).
3. I. E. Sajó, "X-Ray Diffraction Quantitative Phase Analysis of Bayer Process Solids", in *Proceedings of 10th International Congress of ICSOBA (ICSOBA TRAVAUX)*, C.R.C. of Hungarian Academy of Sciences, Bubaneshwar, India, 2008.
4. I.E. Sajó, *XDB Powder Diffraction Phase Analytical System*, Version 3.0, User's Guide, Budapest, 2005.
5. W. Bale, E. Bélisle, P. Chartrand, S. A. Decterov, G. Eriksson, K. Hack, I. H. Jung, Y. B. Kang, J. Melançon, A. D. Pelton, C. Robelin and S. Petersen, "FactSage Thermochemical Software and Databases - Recent Developments", *Calphad*, **33** 295-311 (2009).